

# Effect of Curve Angle on Single Cell Box-Girder Bridge

Preeti Agarwal<sup>1,\*</sup>, Priyaranjan Pal<sup>2</sup>, Pradeep Kumar Mehta<sup>3</sup>

<sup>1</sup> Department of Civil Engineering, Research Scholar, Motilal Nehru National Institute Technology, Prayagraj, 211004, India

<sup>2</sup> Department of Civil Engineering, Associate Professor, Motilal Nehru National Institute Technology, Prayagraj, 211 004, India

<sup>3</sup> Department of Civil Engineering, Professor, Motilal Nehru National Institute Technology, Prayagraj, 211 004, India

Paper ID - 050013

## Abstract

The behaviour of curved box-girder bridge is quite different from the straight one as it is experienced by the additional torsional moments. The analysis and design of such box-girder bridges are quite complicated when the curve angle is varied. The effect of curve angle on the forces and deflection in the girders, inner and outer, of a simply supported single cell reinforced concrete curved box-girder bridge is investigated in this study. A Finite element based software, CSiBridge v.20, was used for the analysis. A convergence study was performed on the proposed model to select the optimum mesh size and the results obtained are validated with the published literature. The variation of absolute values of forces and deflection along both the girders, under dead load (DL) and IRC (Indian Road Congress) live load (LL), is observed and the equations are proposed for their prediction in terms of non-dimensional parameters, using the statistical approach. The present results may be helpful to the designers in the analysis and design of curved single cell reinforced concrete box-girder bridges.

**Keywords:** Box-girder bridge, Single cell, Curve angle, IRC loading, FEM

## 1. Introduction

Box-girder bridge has a cellular cross-section that resists the high torsional moment and becomes more economical when the deck of the bridge is curved in plan (Fig. 1). Previously, bridges with curved layout were unusual; however, most of the straight bridges were curved with the issue of site constraint, alignment construction, higher traffic and velocity limit changes. The analysis and design of curve bridges are more difficult as they are subjected to both bending and torsion. The effect of curve angle on small curvature bridges can be ignored if they are within the permissible limit. Because of the availability of a high-capacity computing system, today it becomes easy to handle the analysis and design of curved bridges with more curvature.

Many studies on the curved bridges are available in the literature, and this section includes a few of them. Barr et al. [1] analysed the effect of diaphragms, lifts and curve angle to determine the distribution factors on pre-stressed concrete girder bridges. Samaan et al. [2] used the finite element method to determine the natural frequencies of continuous curved composite multiple-box girder bridges. Khaloo and Kafimosavi [3] determined the stresses under dead and pre-stress load on each web of curved pre-stressed (post-tensioned) box girder bridges using three-dimensional refined finite-element method. Samaan et al. [4] studied the shear force, stresses, deflection and reaction in curved

continuous composite multiple box-girder bridges under AASHTO (American Association of State Transportation Officials) truck load. Kim et al. [5] used the finite element method to determine the girder distribution factors (GDF) for the moment. The different parameters like curvature, cross-section, span and girder spacing were used for determining the effects. Cho et al. [6] determined the load distribution factor using the finite element method in pre-stressed concrete (PSC) girder bridges. Then, this load distribution factor compared with the AASHTO LRFD, AASHTO Standard factors results. Arici et al. [7] suggested a method of Hamiltonian structural analysis to determine the effect of torsion on steel box and I-girder bridges. The different parameters like loading condition, curvature, cross-section etc. were used in the study. Kim et al. [8] analysed the precast PSC curved girder bridges with multi-tasking formwork with different curvatures. The safety and serviceability of the precast PSC curved bridges are increased when the multi-tasking formwork is used for construction. Gupta and Kumar [9] determined the absolute bending moment of a simply supported reinforced concrete (RC) skew-curved box-girder bridge under dead and IRC 70R tracked vehicle loads, using FEM (finite element method). Gupta et al. [10] evaluated the fundamental frequency of single, double and triple cells RC curved box-

\*Corresponding author. Tel: +919634951210; E-mail address: [gotopreetiagarwal@gmail.com](mailto:gotopreetiagarwal@gmail.com)

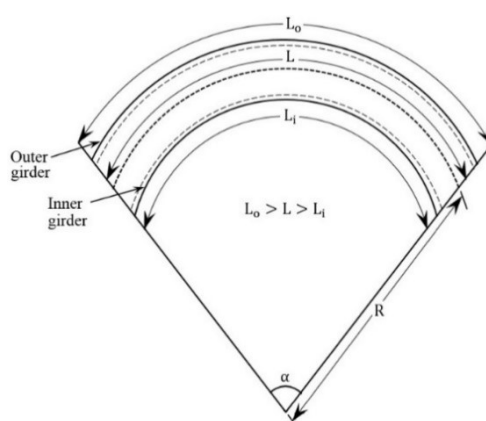


Fig. 1. Curved box-girder bridge deck

girder bridges using finite element analysis. Agarwal et al. [11] investigated the maximum bending moment and shear force in a single cell skew box-girder bridge using the finite element based software SAP2000 and the effect of span, girder spacing and span-depth ratio on bending moment and shear force are observed. Gupta et al. [12] determined the effect of curve angle on the maximum bending moment, shear force, torsional moment and vertical deflection for the girders of single cell, double cell and triple cell (different cross-sectional area) box-girder bridges under the dead and IRC Class 70R track loads. Agarwal et al. [13] investigate the effect of different parameters i.e., skew angle span, span-depth ratio and girder spacing on maximum bending moment, shear force, torsional moment, stresses and deflection on both the girders of bridges due to combined dead and live loads using finite element based SAP2000 software. Agarwal et al. [14] also investigated the effect of skew and curve angles on the bending moment, shear force, torsional moment and vertical deflection of skew-curved box-girder bridge using finite element method. Most of the researchers have studied the composite curved bridges under AASTHO loadings; only a few literature are available on reinforced concrete bridges. Also, it appears that there is just a couple of studies available on the Indian standard loading. The aim of the study is focused on investigating the effect of curve angle on bending moment (BM), shear force (SF), torsional moment (TM) and vertical deflection (VD) of both the girders of box-girder bridge under the dead load (DL) and IRC (Indian road congress) Class-70 R track loading as live load (LL). It has been found that the effect of curve angle on the forces and deflection is negligible up to  $12^\circ$ ; thus, such bridges may be analysed and designed as a straight one. Under both DL and LL, the forces and deflection in the outer girder of the deck is influenced more by the curve angle and are found to be increased with the curve angle, while in case of inner girder, these are found to be decreased with the increase in curve angle. A few equations are proposed to evaluate the bending moment

ratio (BMR), the shear force ratio (SFR), the torsional moment ratio (TMR) and the vertical deflection ratio (VDR) under both dead and live loads in both the girders of box-girder bridges by using the statistical approach. Herein, the BMR is the ratio of maximum BM for any curve angle ( $\alpha$ ) to the maximum BM for a straight bridge. Other ratios SFR, TMR and VDR are defined similarly in the study to obtain the effects of curve angle on the BMR, SFR, TMR, and VDR. These equations may be useful for the designers as they can quickly evaluate curved bridges' responses with the help of any span of a straight bridge under both dead and live loads.

## 2. Modelling Process and Validation

An existing model of single cell box-girder bridge, presented by Gupta and Kumar (2018), is considered to validate the present modelling process. The cross-sectional properties of the existing model are: Span-27.4 m; Width-10.8 m; Overall depth- 2.96 m; Kerb on both sides of deck- 0.2 m; and thickness of top and bottom flanges- 250 mm and 280 mm, respectively. The material properties of concrete considered are: Poisson's ratio = 0.2; Characteristic strength = 25 MPa; Density = 25 kN/m<sup>3</sup>; and Modulus of elasticity =  $2.5 \times 10^7$  kN/m<sup>2</sup>. The model is developed in CSiBridge finite element software and four noded shell element with six degrees of freedom system is used for discretizing the model. The results are found to be converged at 200mm square mesh size. The maximum bending moment (MBM) in the inner and outer girders of box-girder bridge due to DL and LL is calculated and compared with the results reported by Gupta and Kumar [9]. From Figs. 2 and 3, it is clearly seen that the present results are found to be in close agreement. One may say that the present modeling process is appropriate and can be applied with varying parameters for further investigation.

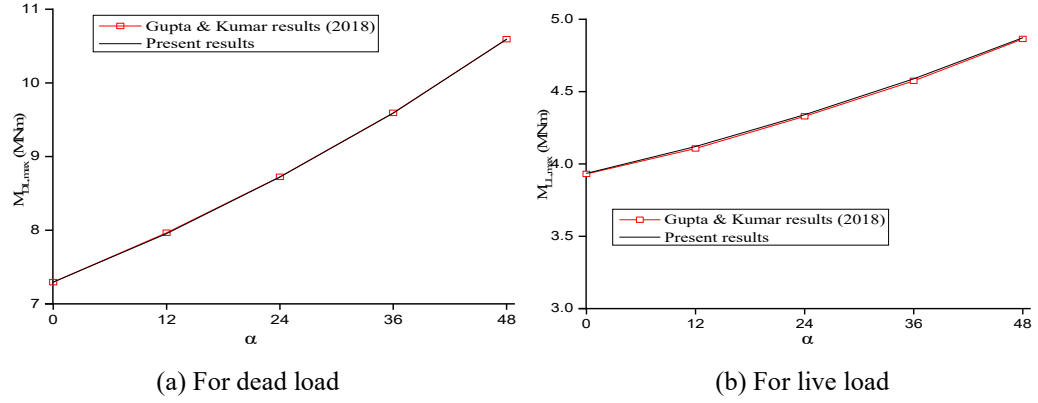


Fig. 2. Variation of MBM with curve angle in outer girder

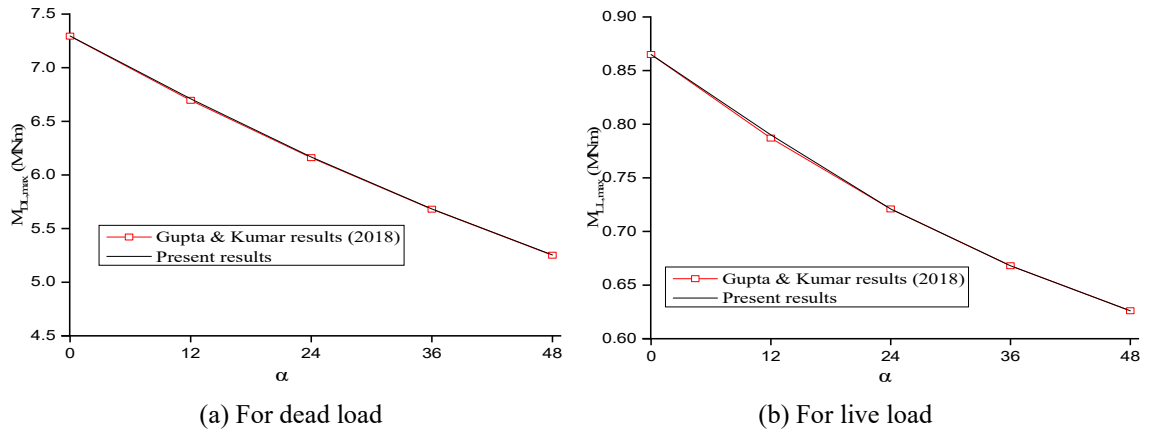


Fig. 3. Variation of MBM with curve angle in inner girder

### 3. Modelling Process and Validation

The effect of curve angle on both the girders of a single cell box-girder bridge is examined. The cross-sectional properties for the bridge considered are: Span-25m, Total width-11.5m (two-lane carriageway-7.5m, kerb-0.5m and footpath-1.5m on both sides), Thickness of top flange ( $t_{tf}$ )-0.3m, Thickness of bottom flange ( $t_{bf}$ )-0.3m, Thickness of web ( $t_w$ )-0.3m, Depth (D)-2.6m and L/d-10. Figure 4 displays the box-girder bridge deck model for the present study. Under limit state of collapse (stress) and serviceability (deflection and vibration), all the straight

bridges are pass. However, the same cross-sections are used in the parametric study of curved bridges.

The material properties of concrete used in the bridge model are: Poisson's ratio = 0.2; Characteristic strength = 40 MPa; Density = 25 kN/m<sup>3</sup>; and Modulus of elasticity =  $3.16 \times 10^7$  kN/m<sup>2</sup>. The material properties of reinforcing steel are: Density = 78 kN/m<sup>3</sup>; Yield strength = 500 MPa; Ultimate tensile strength = 545 MPa and Modulus of elasticity =  $2 \times 10^8$  kN/m<sup>2</sup>.

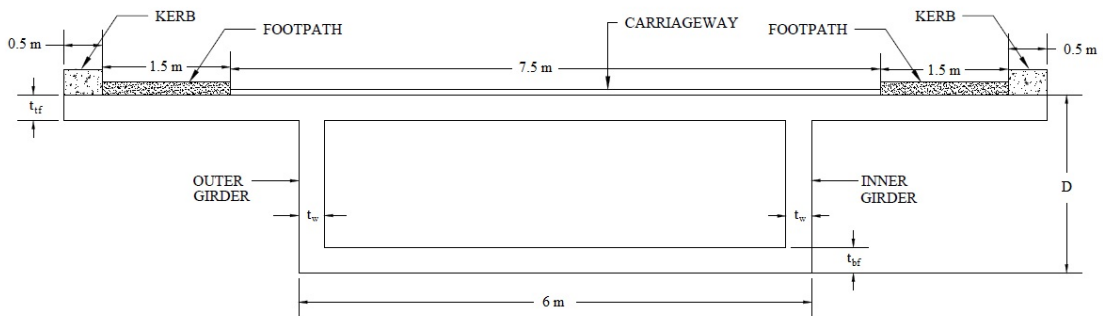


Fig. 4. Model of bridge deck system (dimensions are in meter)

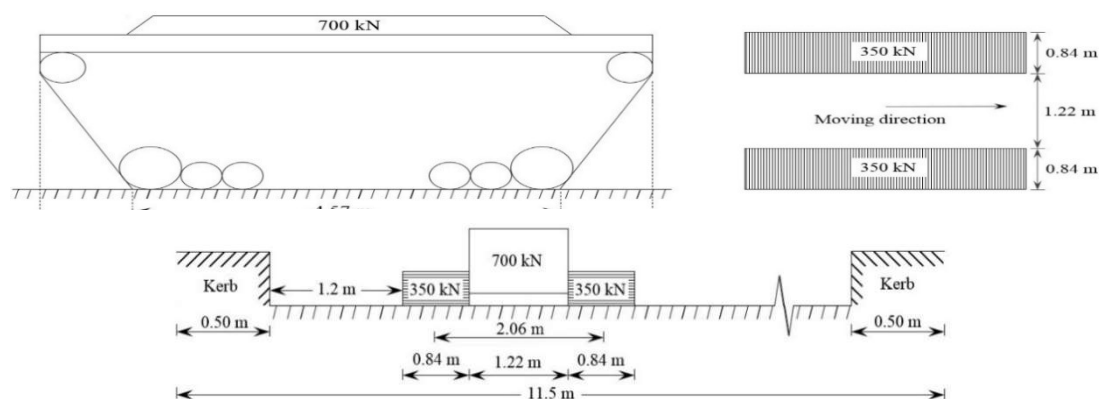
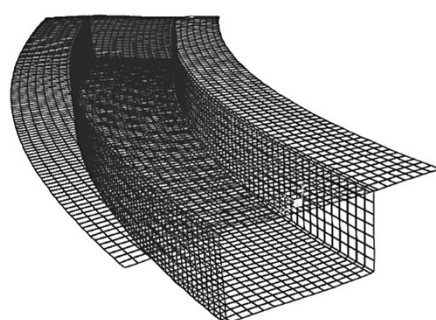
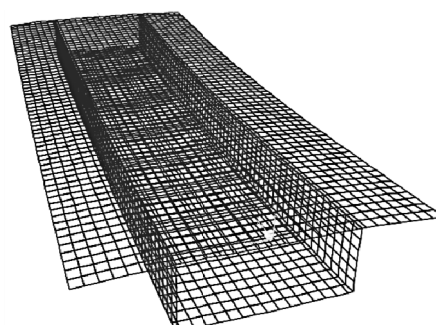


Fig. 5. IRC Class-70R track load


(a) Shell element of curved single cell box-girder bridge ( $\alpha=36^\circ$ )


(b) Shell element of straight single cell box-girder bridge

Fig. 6. Finite element model of box-girder bridge

The following are assumed in the analysis: Material is elastic and homogeneous; Deck rests on two longitudinal girders, and the deck is simply supported; Two end diaphragms are provided in all the bridge models; Effects of kerb, footpath, and super elevation are neglected in all the bridge models; Both dead and live loads are considered as service loads, and other loads such as gravity, wind, seismic, snow, creep, thermal and fatigue are neglected.

At first, all the Indian standard loadings (Class 70R track & wheel load, Class AA track & wheel loads and Class A load) are applied to the bridge model to check which load is producing the more severe condition. Finally, the IRC Class 70R track load is considered in this study because it produces higher stress and deflection. As per IRC-6 specification, this load is applied at a distance of 1.2 m from the kerb face, shown in fig. 5. Simply supported boundary condition is used for the analysis of all bridge deck models. Figure 6 depicts the bridge models, created in finite element based CSiBridge v.20 software. A convergence study is also carried out for these models and it is found that the results are converged at a mesh size of 100 mm. Thus, the mesh size of 100 mm is adopted for the parametric study.

The effect of curve angle on the BM, SF, TM and VD for both the girders of a single cell box-girder bridge under both the loads (DL and LL) is studied. For the investigation, a bridge of 25 m span ( $L$ ) and span-depth ratio ( $L/d$ ) 10 is considered.

### 3.1 Effect of curve angle on the BM

Figure 7 shows the variation of BM in the outer and inner girders of the box-girder bridge for different curve angles under both the DL and LL. These figures clearly reveal that for a straight box-girder bridge, DL-BM is the same along both the girders. In the case of LL, the BM is found to be higher along the inner girder in comparison to that of the outer girder because the LL is placed close to the inner girder. For the outer girder, BM increases considerably with the increase in curve angle in comparison to that in the straight bridge for both DL and LL because of the longer length of the outer girder in comparison to the inner girder. However, it decreases significantly in the case of inner girder under both the DL and LL. The increase in DL-BM for the outer girder is found to be about 10, 19, 30, 45, and 60% for curve angles of 12, 24, 36, 48 and 60°, respectively, compared to those in the straight bridge. For the inner girder, it decreases by about 6, 12, 19, 23 and 27%. However, the LL-BM for the outer girder increases by about 7, 13, 21, 30 and 40% for curve angles of 12, 24, 36, 48 and 60°, respectively in comparison to the straight bridge. For the inner girder, it decreases by about 4, 8, 11, 14 and 17% for curve angles of 12, 24, 36, 48 and 60°, respectively.

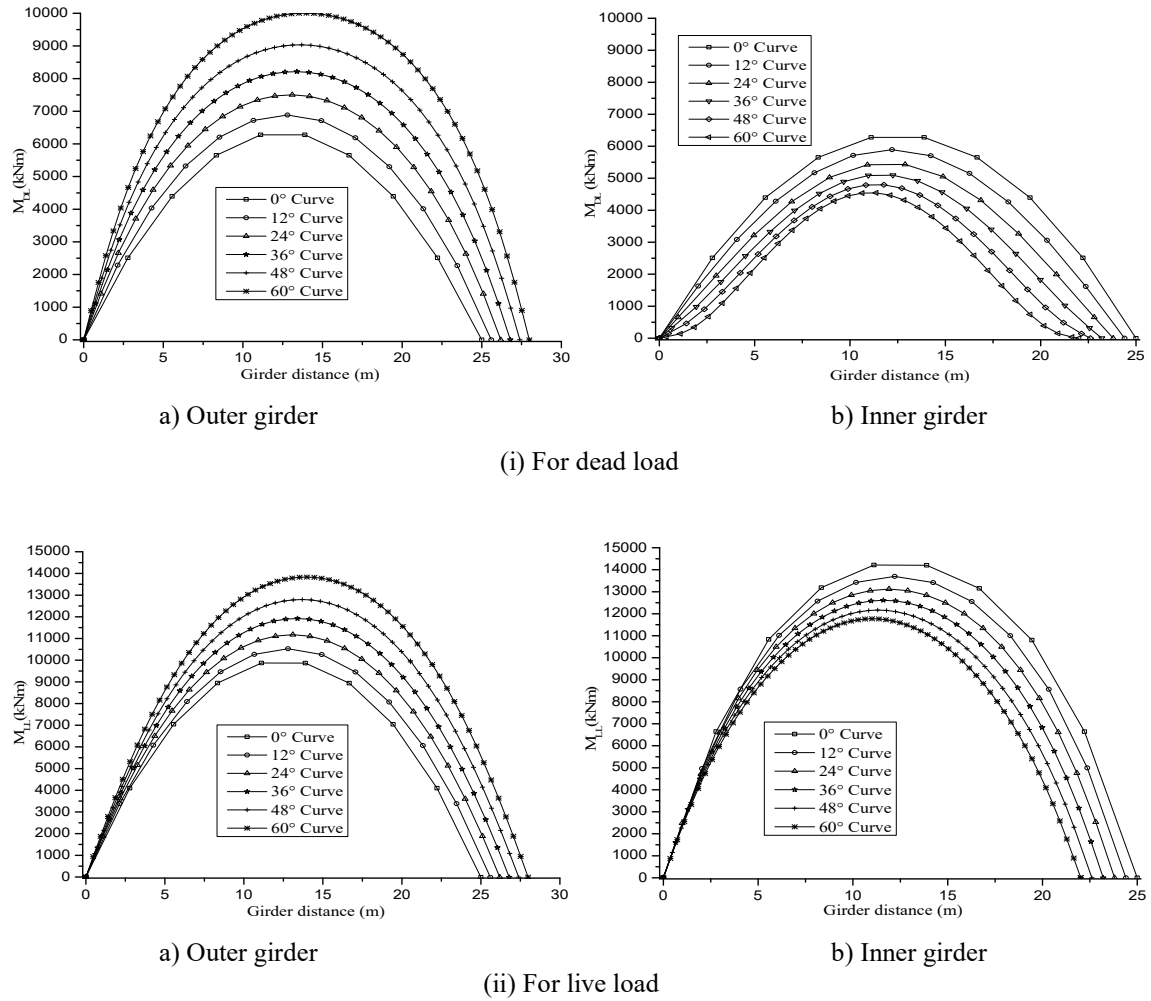


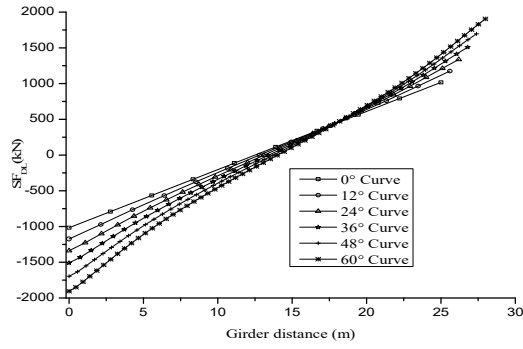
Fig. 7. Variation of curve angle due to variation of DL and LL moment

### 3.2 Effect of curve angle on the SF

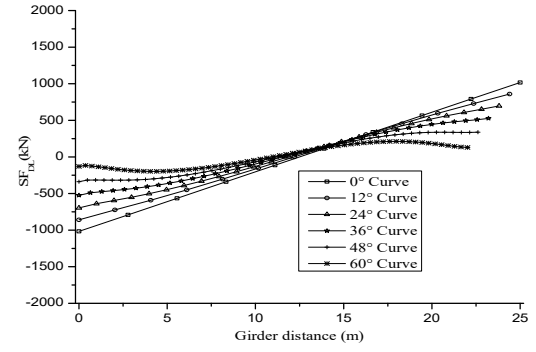
Figure 8 shows the variation of SF along the outer (longer) and inner (shorter) girders of the box-girder bridge with different curve angles for both DL and LL. For the outer girder, it is observed that the SF increases significantly with the curve angle due to both the DL and LL, because of its longer length in comparison to the inner girder. However, for the inner girder, it decreases with the increase in curve angle. The effect of curve angle on the LL-SF is found to be insignificant near the mid-span, but at support, it increases in the outer girder and decreases in the inner girder. The amount of live load is the same for all the models, so the effect is not significant. For the outer girder, the DL-SF increases by about 15, 31, 48, 67 and 87% for curve angles 12, 24, 36, 48 and 60°, respectively in comparison to those in the straight bridge, while the respective changes in the LL-SF are about 3, 7, 10, 16 and 21%. For the inner girder, the DL-SF decreases by about 15, 31, 48, 67 and 79% for curve angles of 12, 24, 36, 48 and 60°, respectively, while for the LL-SF, the respective changes are in the range of about 2-10%.

### 3.3 Effect of curve angle on the TM

Figure 9 shows the effect of curve angle on the TM for both the girders (inner and outer) longitudinally. The TM shows a mixed trend along the length of the girders and it is found to be higher near the ends of the girders. The DL-TM increases with curve angle for the outer girder but it decreases for the inner girder (<60° curve). But, it increases when the curve angle is more than 48°. For the outer girder, the LL-TM increases considerably with curve angle, while for inner girder, it decreases till the mid-span of girder after that it increases. For the outer girder, the DL-TM increases by about 21, 43, 69, 97 and 129% for curve angles 12, 24, 36, 48 and 60°, respectively. While for the inner girder, it decreases by about 16, 29, 43, 37% for curve angles 12, 24, 36 and 48° but it increases by about 3% for a curve angle of 60° in comparison to the straight bridge. For the outer girder, the LL-TM increases by about 4, 6, 8, 20 and 44%, while for the inner girder, it decreases by about 3 to 15%.

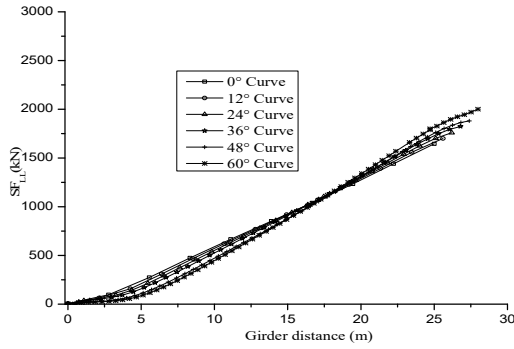


a) Outer girder

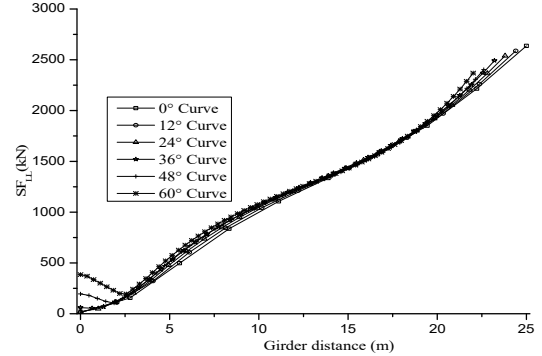


b) Inner girder

(i) For dead load



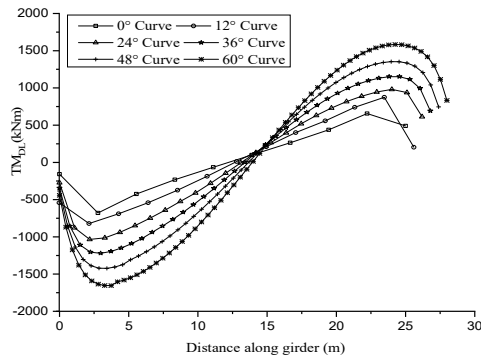
a) Outer girder



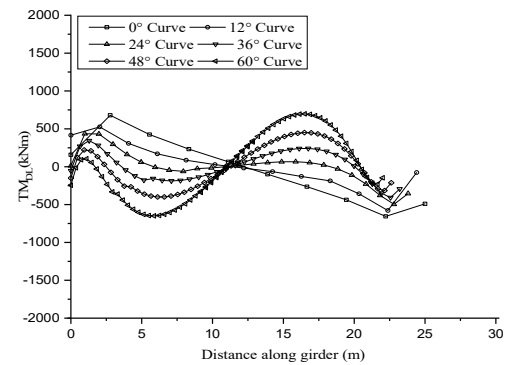
b) Inner girder

(ii) For live load

Fig. 8. Variation of curve angle on variation of DL and LL shear force

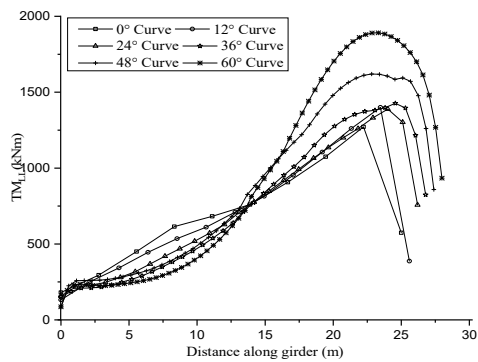


a) Outer girder

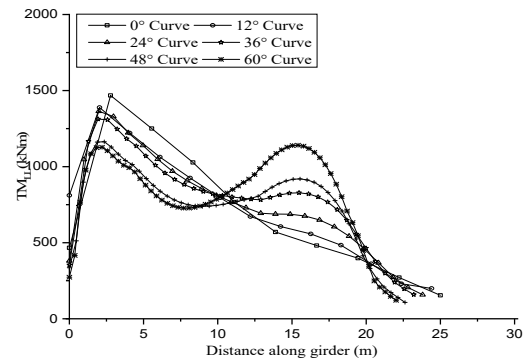


b) Inner girder

(i) For dead load



a) Outer girder



b) Inner girder

(ii) For live load

Fig. 9. Variation of curve angle on variation of DL and LL torsional moment

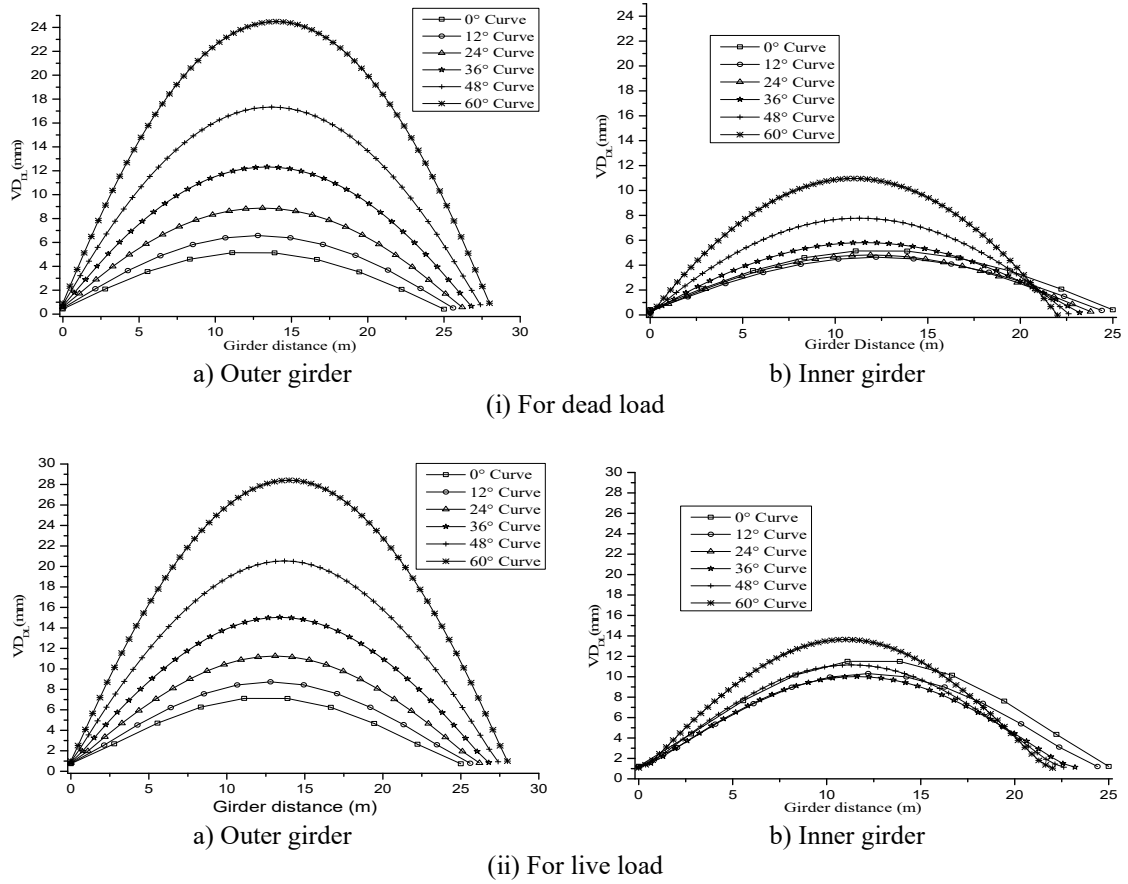


Fig. 10 Variation of curve angle on variation of deflection due to DL and LL

### 3.4 Effect of curve angle on the deflection

Figure 10 shows the variation of vertical deflection due to DL and LL in both the girders. For a smaller curve angle up to 12°, no significant results are found for the VD. The DL-VD increases with curve angle for the outer girder, while for the inner girder, it decreases till a curve angle of 24° and then after increases. The LL-VD increases with curve angle for the outer girder while it decreases up to 48°. For the outer girder, the DL-VD increases by about 28, 73, 139, 237 and 377% for curve angle 12, 24, 36, 48 and 60°, respectively, in comparison to the values of a straight bridge, while for the inner girder it decreases by about 10 and 6 % for curve angle 12 and 24° but it increases by about for curve angle for 36, 48 and 60°, respectively. For the outer girder, the LL-VD increases by about 22, 58, 111, 188 and 299% for curve angle 12, 24, 36, 48 and 60°, respectively, in comparison to the values of a straight bridge, while for the inner girder it decreases by about 3 to 15% for curve angle 12 to 48° but it increases by about 18% for curve angle 60°.

### 3.5 Proposed equations for forces and deflection

To determine the effect of bending moment ratio (BMR), shear force ratio (SFR), torsional moment ratio (TMR) and vertical deflection ratio (VDR) in the outer and inner girders under the primary loads (DL and LL). The higher order terms

are used to get an accuracy in the equations. Some of the equations are proposed which are as follows:

1. Under dead load:

(i) For outer girder:

a) The BMR is

$$BMR_{DL(o)} = 1 + 0.00948\alpha, r = 0.995 \quad (1)$$

b) The SFR is

$$SFR_{DL(o)} = 1 + 0.0142\alpha, r = 0.998 \quad (2)$$

c) The TMR is

$$TMR_{DL(o)} = 1.00294 + 0.01566\alpha + 9.75509 \times 10^{-5} \alpha^2, r = 0.999 \quad (3)$$

d) The VDR is

$$VDR_{DL(o)} = 1 + 0.06714\alpha + \sin(\alpha), r = 0.999 \quad (4)$$

(ii) For inner girder:

a) The BMR is

$$BMR_{DL(i)} = 1 - 0.00484\alpha, r = 0.996 \quad (5)$$

a) The SFR is

$$SFR_{DL(i)} = 1 - 0.0132\alpha, r = 0.999 \quad (6)$$

b) The TMR is

$$TMR_{DL(i)} = 1 - 0.01289\alpha + 9.51784 \times 10^{-10} \alpha^5, r = 0.997 \quad (7)$$

Table-1. Verification of the results from the proposed equation

Factor	Girder	Curve angle (deg)	For dead load			For live load		
			Using FEM	Using proposed equation	% variation	Using FEM	Using proposed equation	% variation
BM (kNm)	Outer	60	10000	9850	1.53	13834	13720	0.95
	Inner	60	4549	3227	2.05	11774	11639	1.15
SF (kN)	Outer	48	1696	1710	0.83	1903	1912	0.47
	Inner	48	337	340	0.89	2411	2426	0.62
TM (kNm)	Outer	36	-	-1221	0.02	-	-1479	-0.95
	Inner	36	1220	408	4.77	1465	1343	2.32
VD (mm)	Outer	24	8.88	8.76	1.35	11.25	11.38	1.11
	Inner	24	4.82	4.71	2.19	9.75	9.65	1.01

c) The VDR is

$$VDR_{DL(i)} = 1 + 0.02203\alpha + 0.67491\sin(\alpha), r = 0.999(8)$$

2. Under live load:

(i) For outer girder:

a) The BMR is

$$BMR_{LL(o)} = 1 + 0.00648\alpha, r = 0.995 \quad (9)$$

b) The SFR is

$$SFR_{LL(o)} = 1 + 0.00339\alpha, r = 0.985 \quad (10)$$

c) The TMR is

$$TMR_{LL(o)} = 1 + 2.01654 \times 10^{-5} \alpha^3, r = 0.992 \quad (11)$$

d) The VDR is

$$VDR_{LL(o)} = 1 + 0.02019\alpha + 8.26508 \times 10^{-6} \alpha^3, r = 0.999(12)$$

(ii) For inner girder:

a) The BMR is

$$BMR_{LL(i)} = 1 - 0.00302\alpha, r = 0.998 \quad (13)$$

b) The SFR is

$$SFR_{LL(i)} = 1 - 0.00166\alpha, r = 0.996 \quad (14)$$

c) The TMR is

$$TMR_{LL(i)} = 1 - 0.00236\alpha, r = 0.971 \quad (15)$$

d) The VDR is

$$VDR_{LL(i)} = 1 - 0.01317\alpha + 2.7044 \times 10^{-4} \alpha^2, r = 0.995 \quad (16)$$

Some of the results due to the effect of curve angle on the BM, SF, TM and VD at inner and outer girders of a single cell box-girder bridge under the dead and live loads obtained from the analysis are presented in Table 1 for the validation of the proposed equations. In all the cases, the outcomes deduced from the equations are seen to be very similar to that of the values of the finite element results. Thus, the proposed equations may be used to predict the forces and deflection in a curved box-girder bridge with ease.

## 4. Conclusions

An investigation was carried out to access the behavior of a single cell curved box-girder bridge under the DL and LL. From the obtained results, the following conclusions are drawn:

- The influence of curve angle is not effective up to  $12^\circ$ , so the small curvature bridges can be treated as the straight one.
- For the outer girder, the BM increases considerably with curve angle under both the DL and LL; however, it decreases significantly for the inner girder.
- For the outer girder, the SF increases significantly with curve angle under DL, while it decreases for inner girder and the effect of LL is insignificant for both the girders.
- For the outer girder, the TM increases with curve angle under DL and LL, while, in the case of the inner girder, it decreases.
- For the outer girder, the VD increases considerably with curve angle under both the DL and LL. However, it decreases for inner girder up to curve angle  $24^\circ$  and  $48^\circ$  due to DL and LL, respectively.

## Acknowledgment

The authors acknowledge Motilal Nehru National Institute of Technology Allahabad for providing financial support under TEQIP- III.

## Disclosures

Free Access to this article is sponsored by SARL ALPHA CRISTO INDUSTRIAL.

## References

1. Barr PJ, Eberhard MO, Stanton JF. Live-load distribution factors in prestressed concrete girder bridges. *Journal of Structural Engineering*, 2001; 6(5):298-306.
2. Samaan M, Kennedy JB, Sennah K. Dynamic analysis of curved continuous multiple-box girder bridges. *Journal of Bridge Engineering*, 2007;12(2):184-93.
3. Khaloo AR, Kafimosavi M. Enhancement of flexural design of horizontally curved prestressed bridges. *Journal of Bridge Engineering*, 2007;12(5):585-90
4. Samaan M, Kennedy JB, Sennah K. Impact factors for curved continuous composite multiple-box girder bridges. *Journal of Bridge Engineering*, 2007; 12(1): 80-8.
5. Kim WS, Laman JA, Linzell DG. Live load radial moment distribution for horizontally curved bridges. *Journal of Bridge Engineering*, 2007; 12(6):727-36.
6. Cho D, Park S, Kim W. Live load distribution in prestressed concrete girder bridges with curved slab. *Applied Mechanics Material*, 2013; 284:1441-5.
7. Arici M, Granata MF, Oliva M. Influence of secondary torsion on curved steel girder bridges with box and I-girder cross-sections. *KSCE Journal of Civil Engineering*, 2015;19:2157-71.



8. Kim SJ, Kim JJ, Yi ST, Noor NB, Kim SC. Structural performance evaluation of a precast PSC curved girder bridge constructed using multi-tasking formwork. International Journal of Concrete Structures and Materials, 2016; 10(3):1-17.
9. Gupta T, Kumar M. Flexural response of skew-curved concrete box-girder bridges. Engineering Structure 2018; 163:358-72.
10. Gupta N, Agarwal P, Pal P. Free vibration analysis of RCC curved box girder bridges. International Journal of Technology Innovation in Modern Engineering & Science, 2019; 5:1-7.
11. Agarwal P, Pal P, Mehta PK. Analysis of RC skew box girder bridges. International Journal of Science and Innovative Engineering & Technology, 2019; 6:1-8.
12. Gupta N, Agarwal P, Pal P. Analysis of RCC curved box girder bridges. Applied Innovative Research, 2019; 153-159.
13. Agarwal P, Pal P, Mehta PK. Finite Element Analysis of Skew Box-Girder Bridge. Journal of Structural Engineering (Madras), 2020; 47(3): 243-258.
14. Agarwal P, Pal P, Mehta PK. Parametric study on skew-curved RC box-girder bridges. Structures, 2020; 28: 380-388.
15. IRC 21-2000: Standard specification and code of practice for road bridges, section III-cement concrete (planed and reinforced), 3rd ed.
16. IRC 6-2014: Standard specifications and code of practice for road bridges, section II, loads & stresses.
17. CSiBridge. Analysis Reference Manual Version 20.0.0, Comput Struct Inc., Berkeley, CA.

### List of notation:

$L_o$	Length of outer girder bridge deck	$L_i$	Length of inner girder bridge deck
$L$	Length of central bridge deck	$M_{DL,max}$	Maximum dead load bending moment
$M_{LL,max}$	Maximum live load bending moment	$t_{tf}$	Thickness of top flange
$t_{bf}$	Thickness of bottom flange	$t_w$	Thickness of web
$\alpha$	Curve angle	$BM_{DL}$	Maximum bending moment due to dead load
$BM_{LL}$	Maximum bending moment due to live load	$SF_{DL}$	Maximum shear force due to dead load
$SF_{LL}$	Maximum shear force due to live load	$TM_{DL}$	Maximum torsional moment due to dead load
$TM_{LL}$	Maximum torsional moment due to live load	$VD_{DL}$	Maximum vertical deflection due to DL
$VD_{LL}$	Maximum vertical deflection due to LL	$BMR_{DL(i)}$	Bending moment ratio due to dead load for inner girder
$BMR_{DL(o)}$	Bending moment ratio due to dead load for outer girder	$BMR_{LL(i)}$	Bending moment ratio due to live load for inner girder
$BMR_{LL(o)}$	Bending moment ratio due to live load for outer girder	$SFR_{DL(i)}$	Shear force ratio due to dead load for inner girder
$SFR_{DL(o)}$	Shear force ratio due to dead load for outer girder	$SFR_{LL(i)}$	Shear force ratio due to live load for inner girder
$SFR_{LL(o)}$	Shear force ratio due to live load for outer girder	$TMR_{DL(i)}$	Torsional moment ratio due to dead load for inner girder
$TMR_{DL(o)}$	Torsional moment ratio due to dead load for outer girder	$TMR_{LL(o)}$	Torsional moment ratio due to live load for outer girder
$TMR_{LL(i)}$	Torsional moment ratio due to live load for inner girder	$VDR_{DL(o)}$	Vertical deflection ratio due to dead load for outer girder
$VDR_{DL(i)}$	Vertical deflection ratio due to dead load for inner girder	$VDR_{DL(o)}$	Vertical deflection ratio due to live load for outer girder
$VDR_{LL(i)}$	Vertical deflection ratio due to live load for inner girder	$r$	Correlation coefficient